Electronic Supplementary Material (ESI) for Dalton Transactions.
This journal is © The Royal Society of Chemistry 2015

Electronic Supplementary Information

Redox inactive metal ions triggered *N*-dealkylation by iron catalyst with dioxygen activation: a lesson from lipoxygenases

Jisheng Zhang, Yujuan Wang, Nengchao Luo, Zhuqi Chen, Kangbing Wu, Guochuan Yin*

School of Chemistry and Chemical Engineering, Key Laboratory for Large-Format Battery Materials and System, Ministry of Education, Huazhong University of Science and Technology, Wuhan 430074, PR China;

AUTHOR EMAIL ADDRESS (gyin@hust.edu.cn)

Contents

Figure S1. GC-MS analysis of *N,N*-dimethylaniline oxidation. Reaction conditions: acetonitrile 5 mL, DMA 100 mM, $[Fe(TPA)Cl_2]Cl$ 2 mM, $Zn(OTf)_2$ 4 mM, dioxygen balloon, 313 K, 2 h.

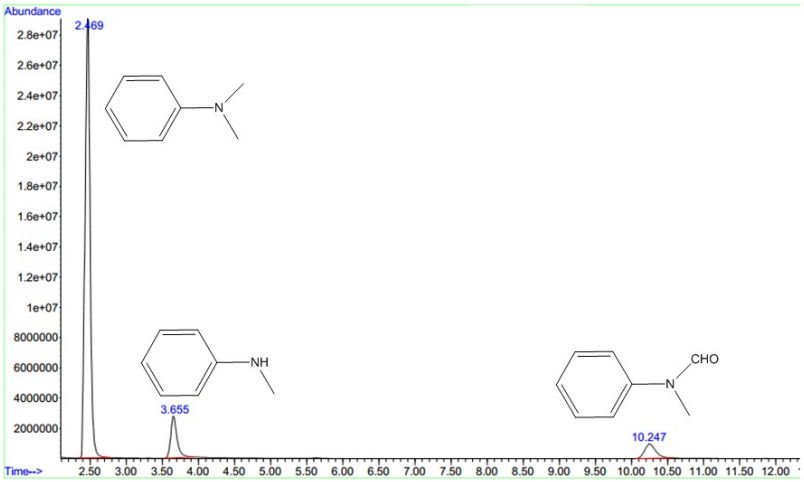

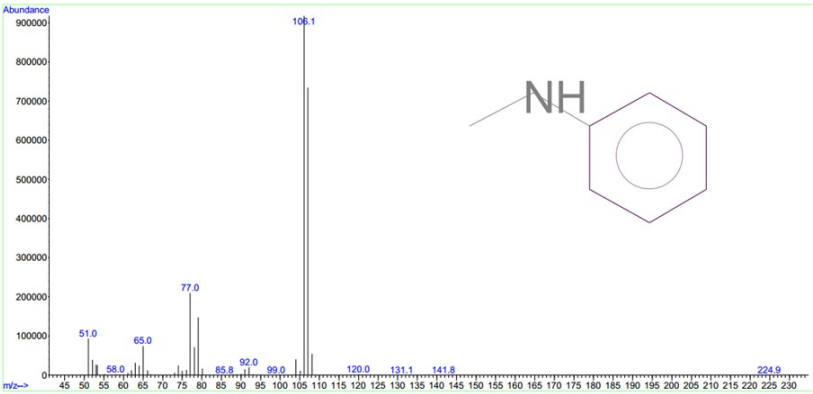

Figure S1-1. Mass spectrum of N-methylaniline product in GC-MS analysis.

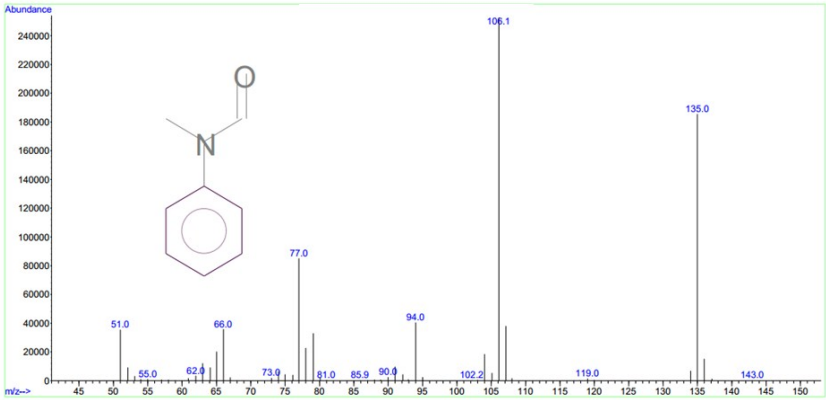

Figure S1-2. Mass spectrum of N-methylformanilide produc in GC-MS analysis.

Figure S2 NMR data of the complicated products of DMA catalyzed by $[Fe(TPA)Cl_2]Cl$ with $Zn(OTf)_2$. Reaction conditions: acetonitrile 100 mL, DMA 100 mM, $[Fe(TPA)Cl_2]Cl$ 2 mM, $Zn(OTf)_2$ 4 mM, dioxygen balloon, 313 K, 10 h.

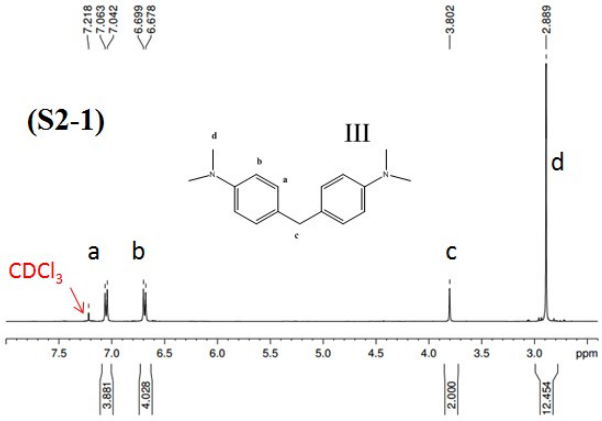

Figure S2-1. ^{1}H NMR spectrum (400 MHz) of isolated 4,4-methylenebis-(*N,N*-dimethylaniline) (**III**) in $CDCl_3$.

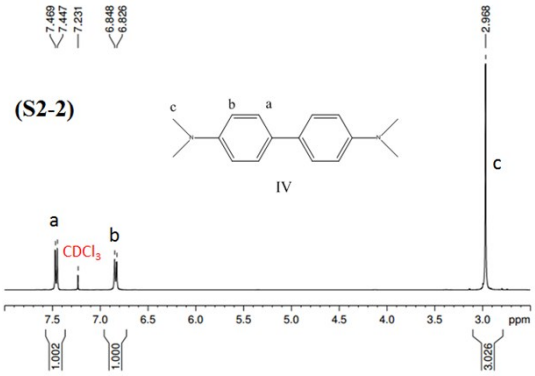

Figure S2-2. ^{1}H NMR spectrum (400MHz) of isolated tetramethylbenzidine (**IV**) in $CDCl_3$.

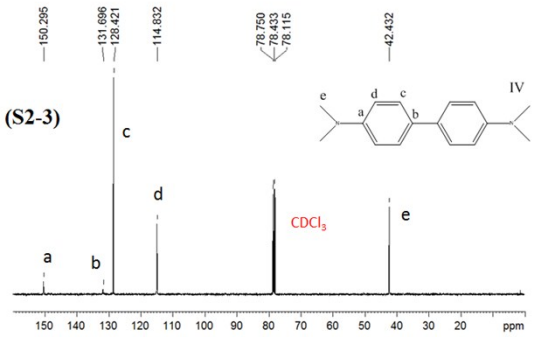

Figure S2-3. ^{13}C NMR spectrum (400 MHz) of isolated tetramethylbenzidine (**IV**) in $CDCl_3$.

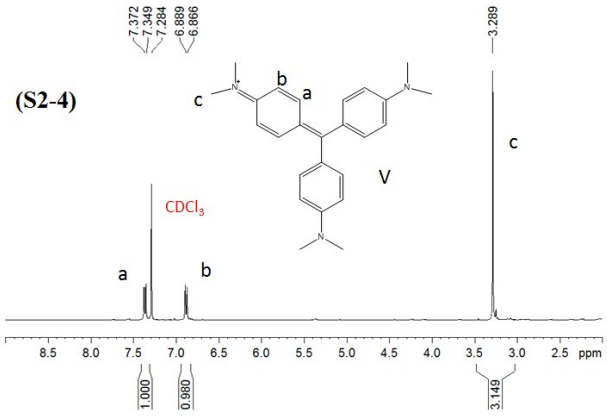

Figure S2-4. ^{1}H NMR spectrum (400 MHz) of isolated trimer (**V**) in $CDCl_3$.

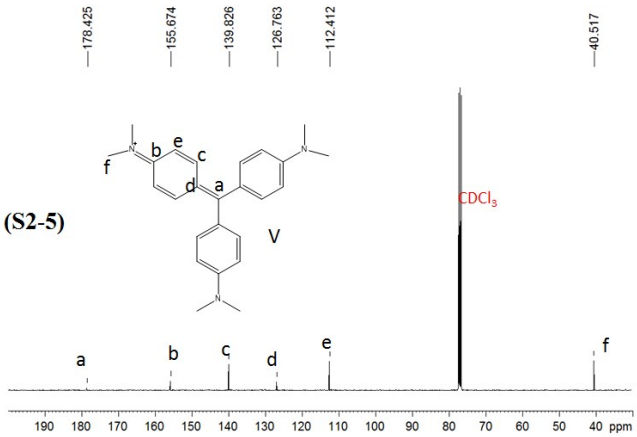

Figure S2-5. ^{13}C NMR spectrum (400 MHz) of isolated trimer (**V**) in $CDCl_3$.

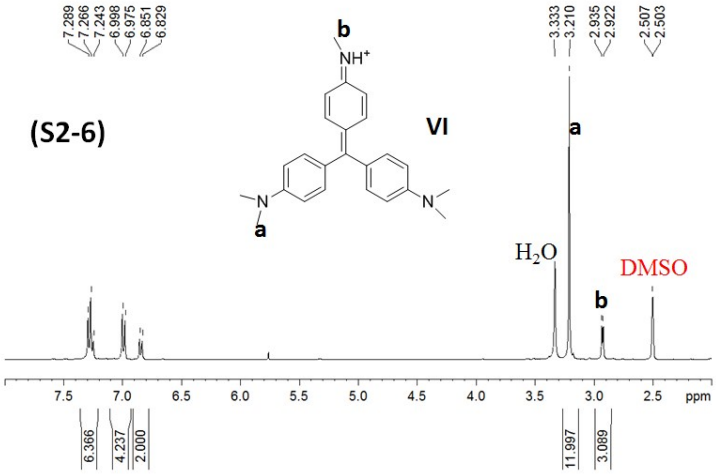

Figure S2-6. ^{1}H NMR spectrum (400 MHz) of isolated trimer (**VI**) in DMSO-d_6.

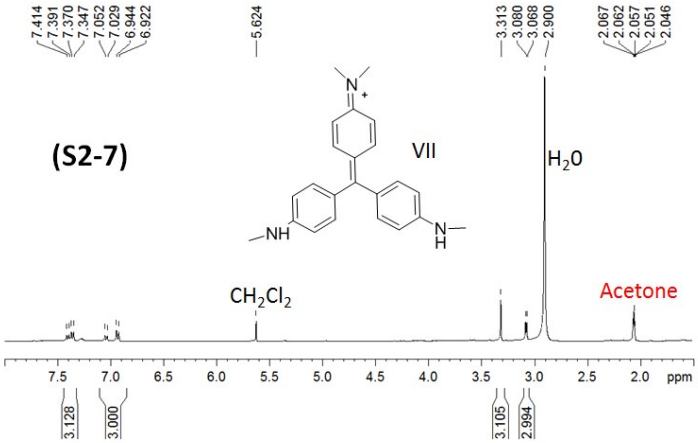

Figure S2-7. ^{1}H NMR spectrum (400 MHz) of isolated trimer (**VII**) in acetone-d_6.

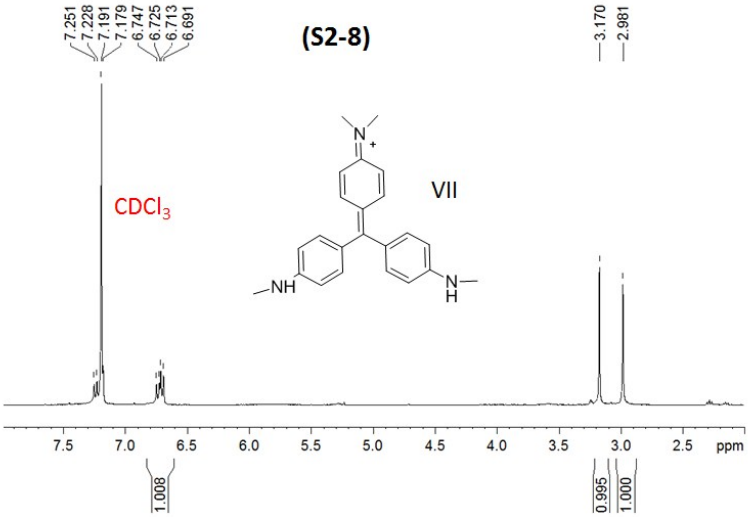

Figure S2-8. ^{1}H NMR spectrum (400 MHz) of isolated trimer (**VII**) in $CDCl_3$.

Figure S3. GC-MS analysis of *p*-Me-DMA oxidation. Reaction conditions: acetonitrile 5 mL, *p*-Me-DMA 100 mM, [Fe(TPA)Cl_2]Cl 2 mM, Zn(OTf)$_2$ 4 mM, dioxygen balloon, 313 K, 2 h.

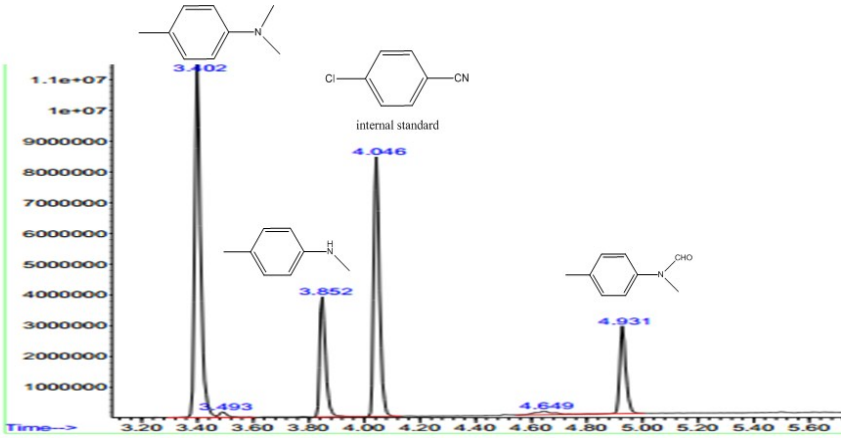

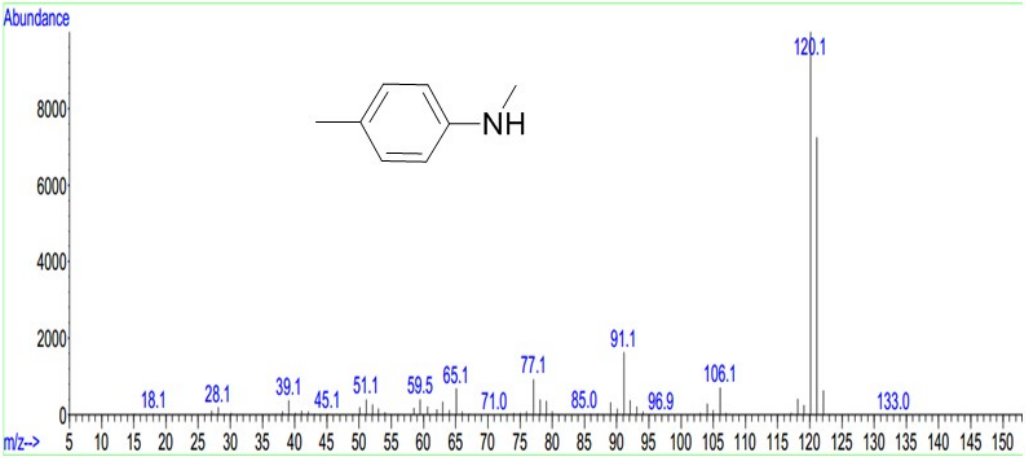

Figure S3-1. Mass graph of *p*-methyl-*N*-methylaniline product in GC-MS analysis.

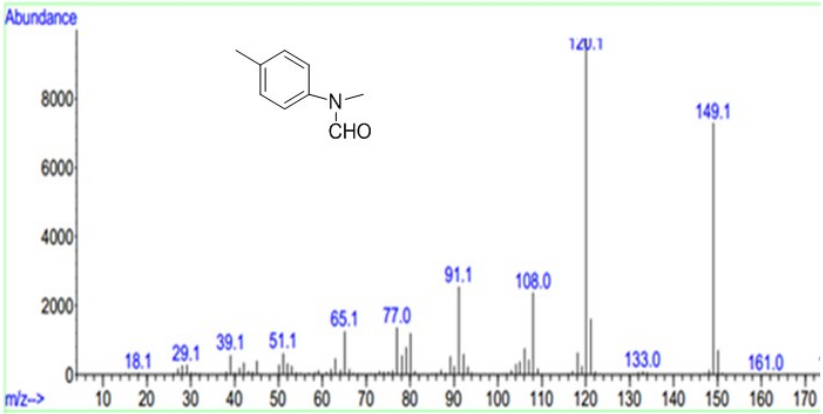

Figure S3-2. Mass graph of *p*-methyl-*N*-methylformamide in GC-MS analysis.

Figure S4. NMR data of N-demethylation and methyl oxidation products of the substituted *N,N*-dimethylanilines. Reaction conditions: acetonitrile 100 mL, substrate 100 mM, [Fe(TPA)Cl_2]Cl 2 mM, $Zn(OTf)_2$ 4 mM, dioxygen balloon, 313 K,10 h.

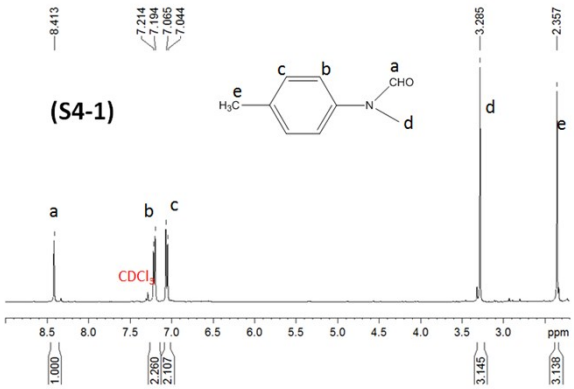

Figure S4-1. ^{1}H NMR spectrum (400 MHz) of isolated *p*-methyl-*N*-methylformamide in $CDCl_3$.

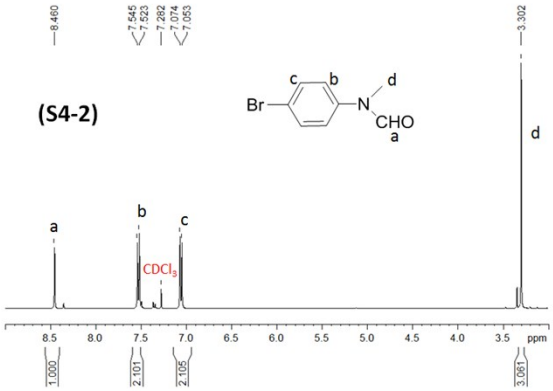

Figure S4-2. ^{1}H NMR spectrum (400 MHz) of isolated *para*-bromo-*N*-methylformanilide in $CDCl_3$.

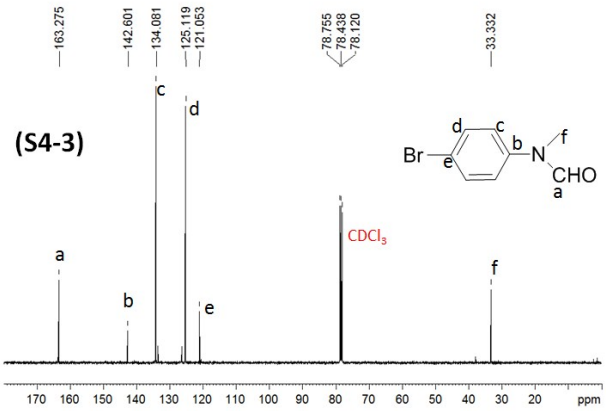

Figure S4-3. ^{13}C NMR spectrum (400 MHz) of isolated *p*-bromo-*N*-methylformanilide in $CDCl_3$.

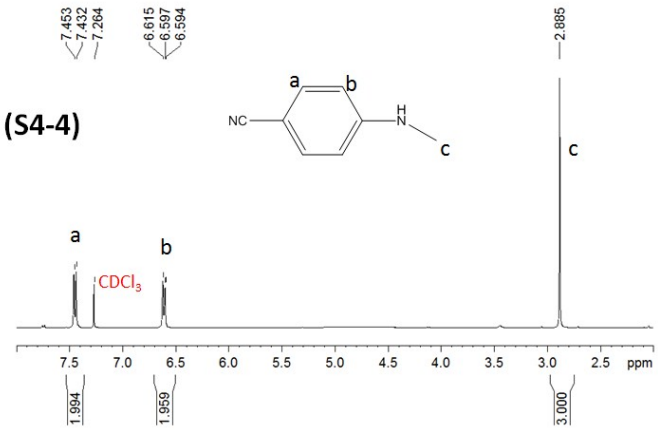

Figure S4-4. ^{1}H NMR spectrum (400 MHz) of isolated *p*-cyano-*N*-methylaniline in $CDCl_3$.

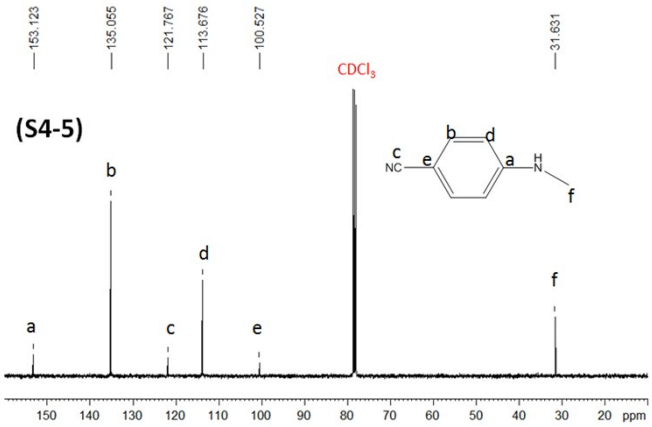

Figure S4-5. ^{13}C NMR spectrum (400 MHz) of isolated *p*-cyano-*N*-methylaniline in $CDCl_3$.

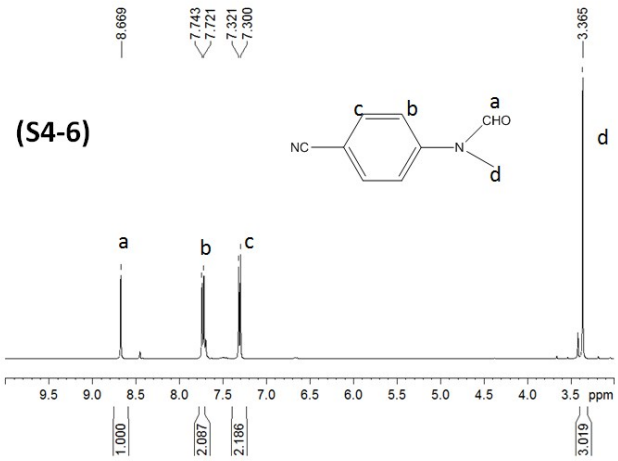

Figure S4-6. ^{1}H NMR spectrum (400 MHz) of isolated *p*-cyano- *N*-methylformanilide in $CDCl_3$.

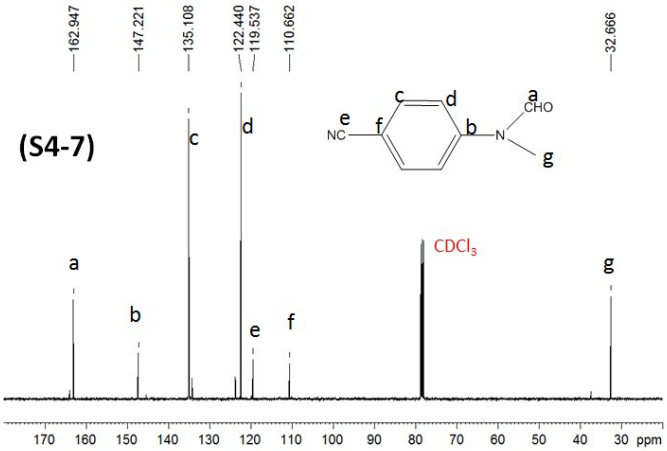

Figure S4-7. ^{13}C NMR spectrum (400 MHz) of isolated *p*-cyano-*N*-methylformanilide in $CDCl_3$.

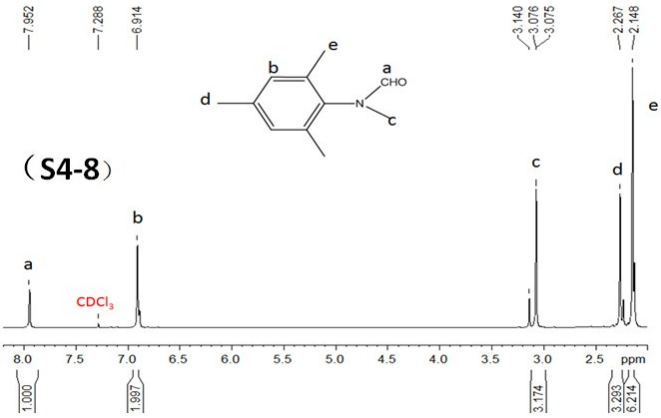

Figure S4-8. ^{1}H NMR spectrum (400 MHz) of isolated methyl group oxidation product from *N,N*,2,4,6-pentamethylaniline in $CDCl_3$.

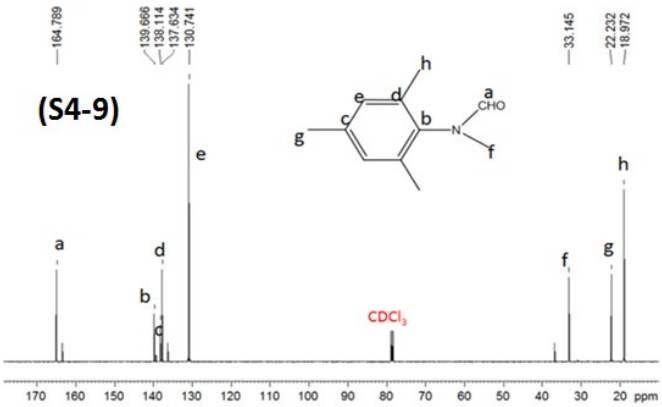

Figure S4-9. ^{13}C NMR spectrum (400MHz) of isolated methyl group oxidation product from *N,N*,2,4,6-pentamethylaniline in $CDCl_3$.

Figure S5. UV-Vis spectra of $[Fe(TPA)Cl_2]Cl$ or $Zn(OTf)_2$ alone with DMA in the control experiments.

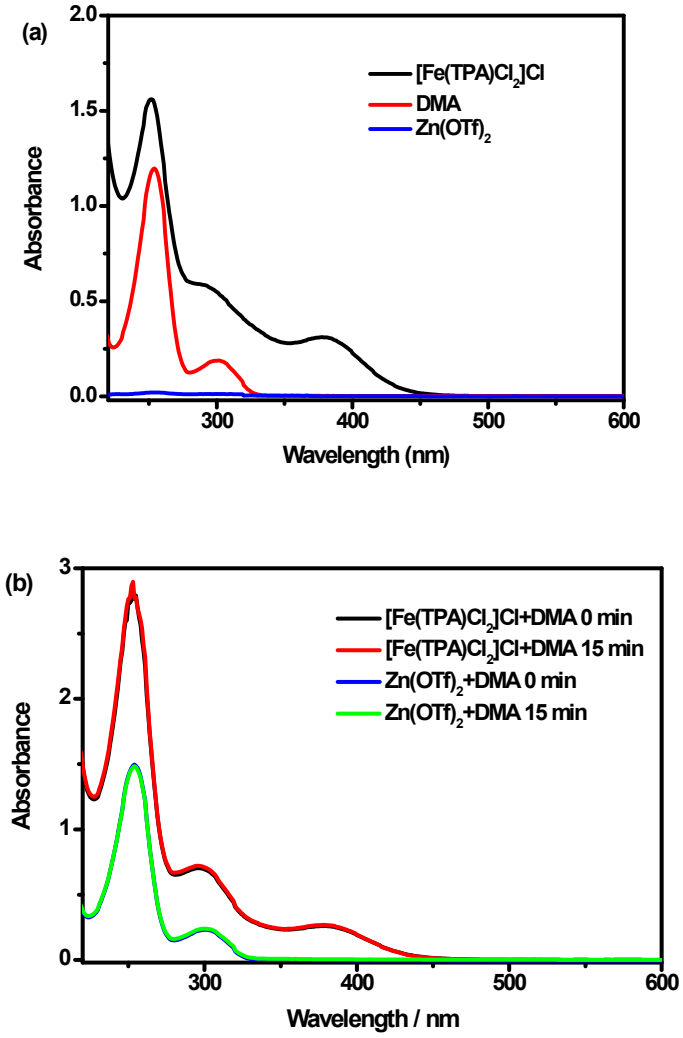

Conditions: solvent, acetonitrile, 298 K. (a) $[Fe(TPA)Cl_2]Cl$ 0.1 mM (black line); DMA 0.1 mM (red line); $Zn(OTf)_2$ 0.2 mM (blue line); (b) $[Fe(TPA)Cl_2]Cl$ 0.1mM, DMA 0.1 mM, 0 min (black line); $[Fe(TPA)Cl_2]Cl$ 0.1 mM, DMA 0.1 mM, 15 min (red line); $Zn(OTf)_2$ 0.2mM, DMA 0.1 mM , 0 min (blue line); $Zn(OTf)_2$ 0.2 mM, DMA 0.1 mM, 15 min (green line).

Figure S6. Mass spectra of (a) $[Fe(TPA)Cl_2]Cl$ 2 mM; (b) stoichiometric reaction solution of $[Fe(TPA)Cl_2]Cl$ 2 mM and $Zn(OTf)_2$ 4 mM with DMA 4mM in acetonitrile.

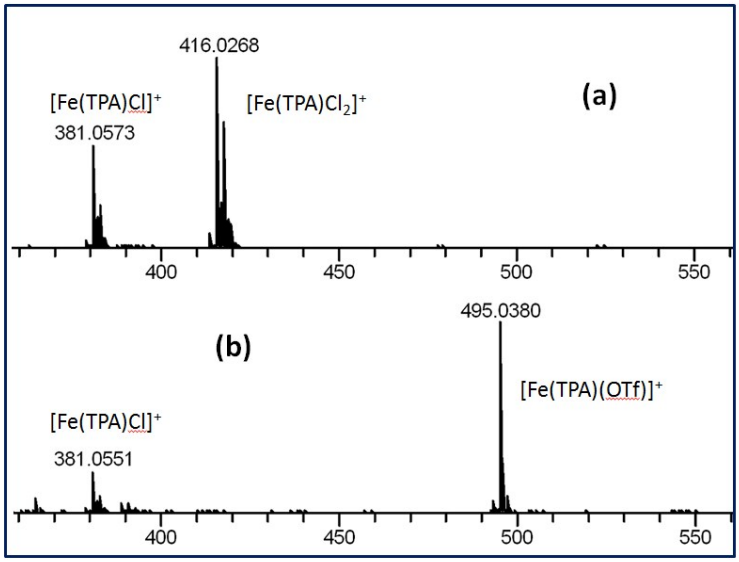

Figure S7. UV-Vis spectrum of ABTS radical cation (cited from reference: Re, R.; Pellegrini, N.; Proteggente, A.; Pannala, A.; Yang, M.; Rice-Evans, C. *Free. Radical. Bio. Med*. **1999**, *26*, 1231-1237.)

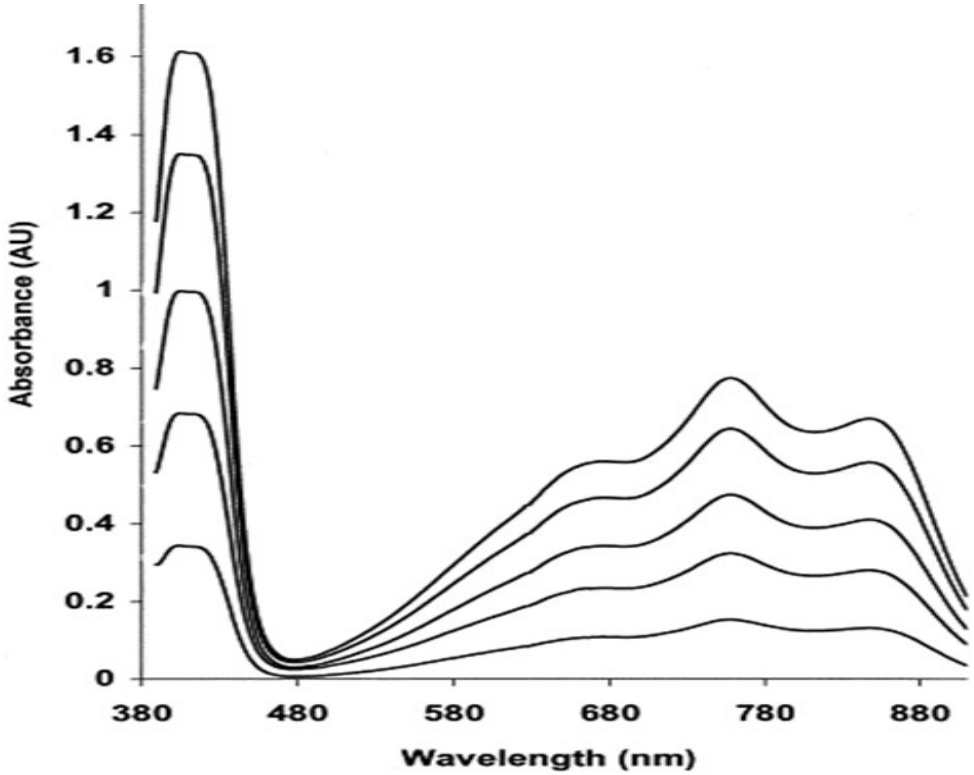

Figure S8. Zn^{2+} triggered electron transfer from ferrocence to $[Fe(TPA)Cl_2]Cl$.

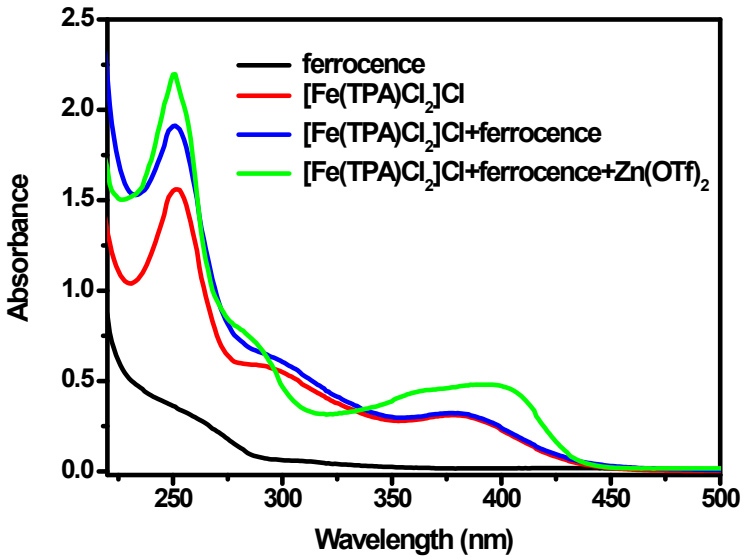

Conditions: solvent, acetonitrile, 298 K. Ferrocence 0.1 mM (black line); $[Fe(TPA)Cl_2]Cl$ 0.1 mM (red line); $[Fe(TPA)Cl_2]Cl$ 0.1 mM, ferrocence 0.1 mM (blue line); $[Fe(TPA)Cl_2]Cl$ 0.1 mM, $Zn(OTf)_2$ 0.2 mM , ferrocence, 0.1 mM (green line).

Figure S9. Kinetics for the oxidation of *p*-Me-DMA catalyzed by $[Fe(TPA)Cl_2]Cl$ or $Fe(TPA)Cl_2$ with $Zn(OTf)_2$.

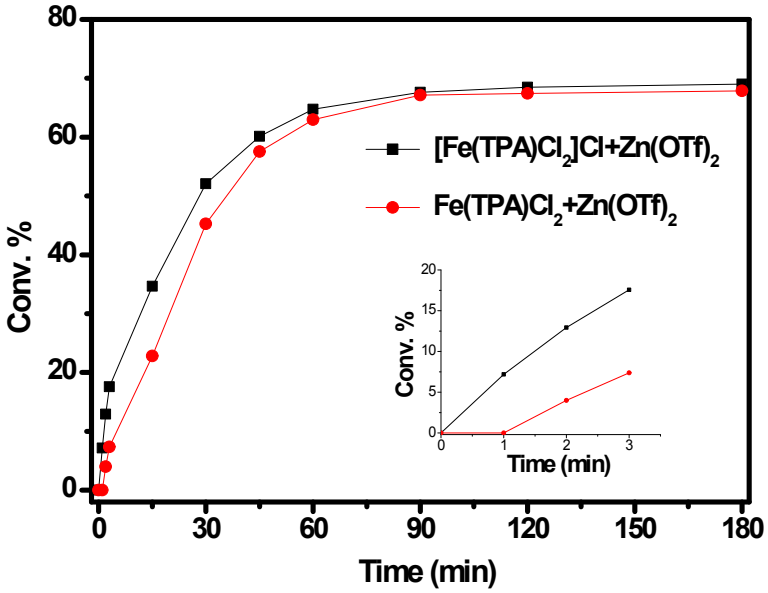

Conditions: acetonitrile 5 mL, *p*-Me-DMA 100 mM, dioxygen balloon, 313 K. $[Fe(TPA)Cl_2]Cl$ 2 mM, $Zn(OTf)_2$ 4 mM (black line); $Fe(TPA)Cl_2$ 2 mM, $Zn(OTf)_2$ 4 mM (red line).

Figure S10. UV-Vis spectra of the acetonitrile solution of $[Fe(TPA)Cl_2]Cl$ with $Zn(OTf)_2$.

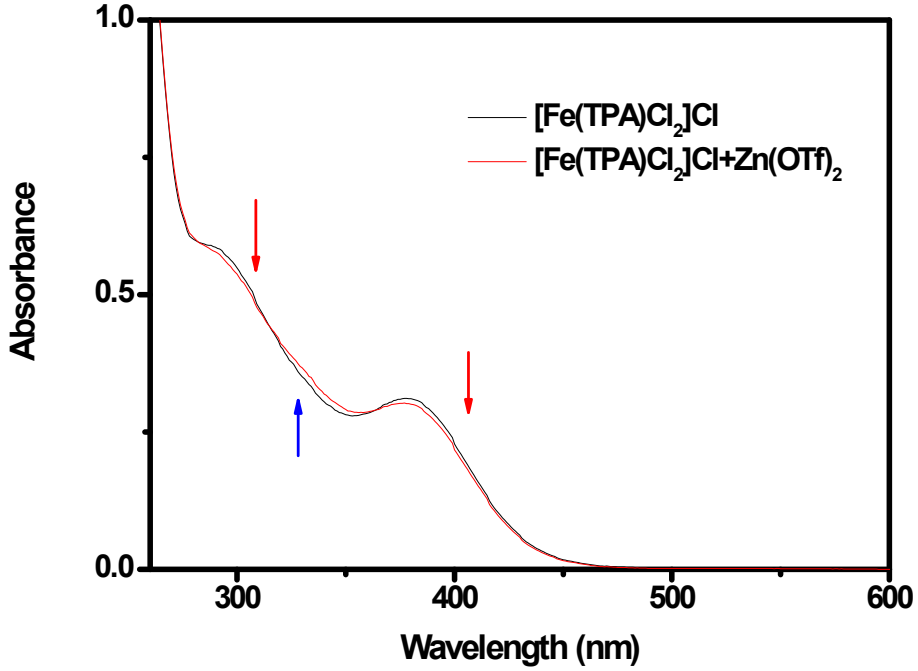

Conditions: solvent, acetonitrile, 298 K. $[Fe(TPA)Cl_2]Cl$ 0.1 mM (black line); $[Fe(TPA)Cl_2]Cl$ 0.1 mM, $Zn(OTf)_2$ 0-0.8 mM.

Figure S11. UV-Vis absorbance change by adding different Lewis acids to $[Fe(TPA)Cl_2]Cl$.

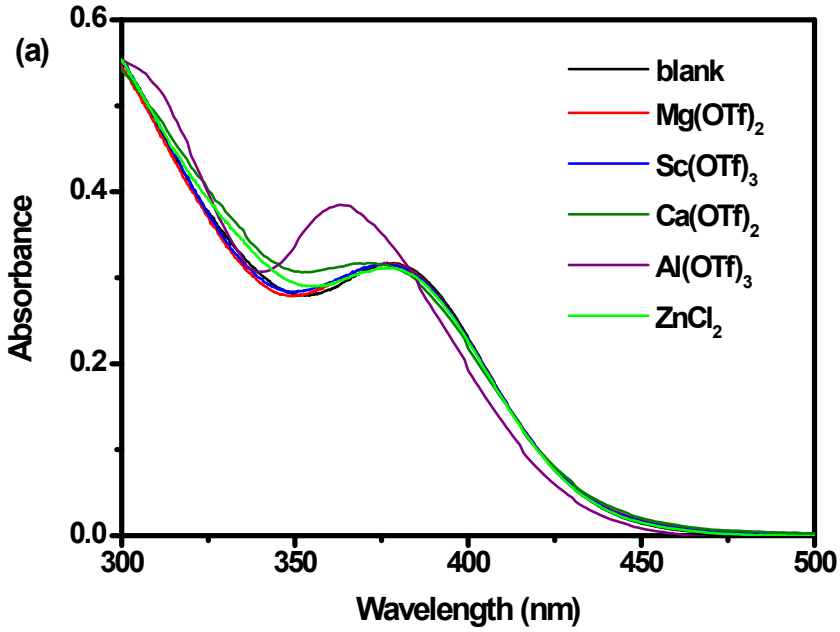

Conditions: solvent, acetonitrile, 298 K. $[Fe(TPA)Cl_2]Cl$ 0.1 mM (black line); $[Fe(TPA)Cl_2]Cl$ 0.1 mM, $Mg(OTf)_2$ 0.2 mM (red line); $[Fe(TPA)Cl_2]Cl$ 0.1 mM, $Sc(OTf)_3$ 0.2 mM (blue line); $Fe(TPA)Cl_2]Cl$ 0.1 mM, $Ca(OTf)_2$ 0.2 mM (olive line); $[Fe(TPA)Cl_2]Cl$ 0.1 mM, $Al(OTf)_3$ 0.2 mM (purple line); $[Fe(TPA)Cl_2]Cl$ 0.1 mM, $ZnCl_2$ 0.2 mM (green line).

Figure S12. Kinetics for the oxidation of DMA catalyzed by[Fe(TPA)Cl_2]Cl with Al(OTf)$_3$ or $ZnCl_2$.

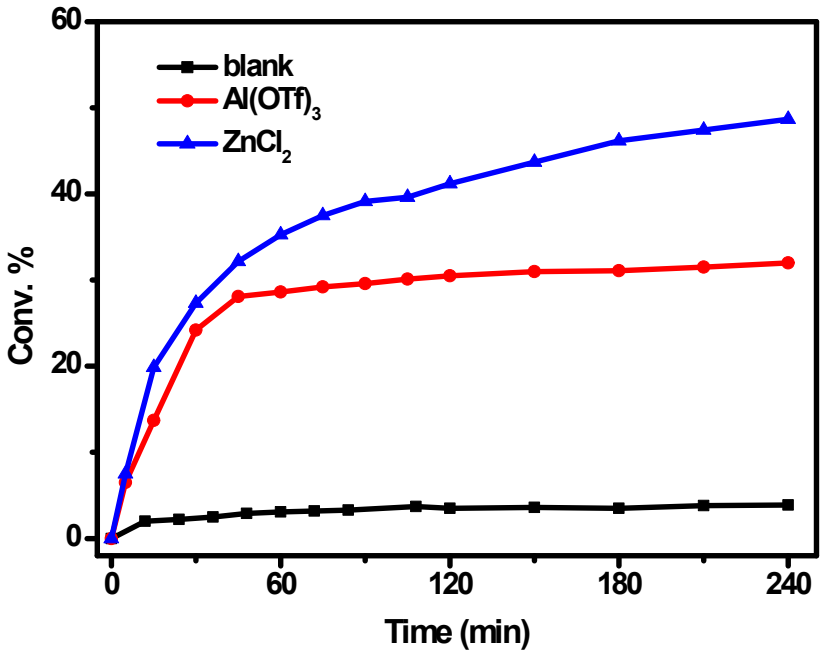

Conditions: acetonitrile 5 mL, DMA 100 mM, dioxygen balloon, 313 K. [Fe(TPA)Cl_2]Cl 2 mM (black line); [Fe(TPA)Cl_2]Cl 2 mM, Al(OTf)$_3$ 4 mM (red line); [Fe(TPA)Cl_2]Cl 2 mM, $ZnCl_2$ 4 mM (blue line).

Figure S13. UV-Vis spectra of the acetonitrile solution of $Fe(TPA)(CH_3CN)_2(OTf)_2$ with $Zn(OTf)_2$.

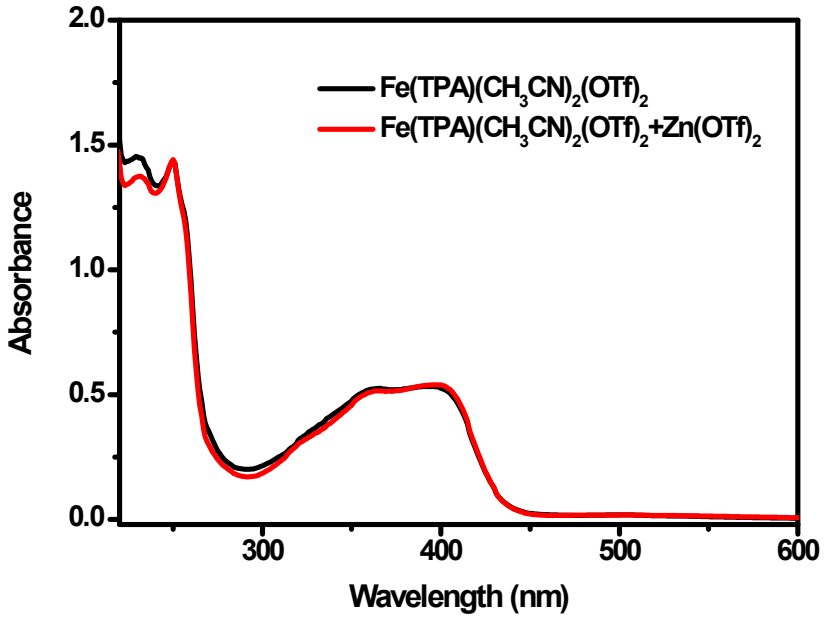

Conditions: solvent, acetonitrile, 298 K. $Fe(TPA)(CH_3CN)_2(OTf)_2$ 0.1 mM (black line); $Fe(TPA)(CH_3CN)_2(OTf)_2$ 0.1 mM, $Zn(OTf)_2$ 0.2 mM (red line).

Figure S14. Mass spectra of (a) $Fe(TPA)(CH_3CN)_2(OTf)_2$ 2 mM , LiCl 2 mM; (b) $Fe(TPA)(CH_3CN)_2(OTf)_2$ 2 mM, LiCl 2 mM, $Zn(OTf)_2$ 4 mM in acetonitrile.

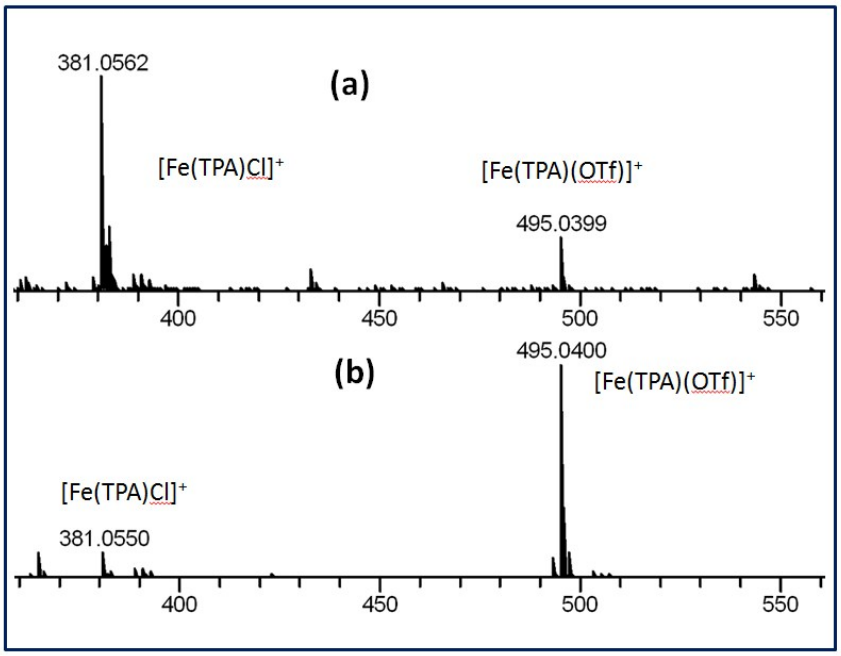

Figure S15. UV-Vis absorbance change of $Fe(TPA)Cl_2$ and $Zn(OTf)_2$ under 1 atm O_2.

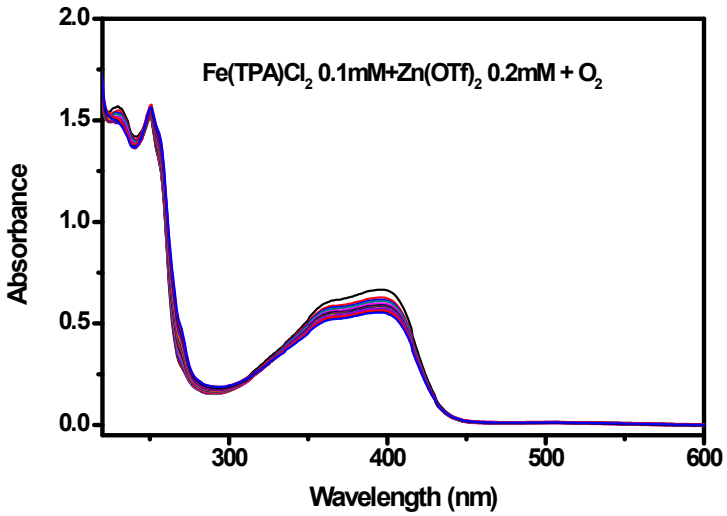

Conditions: solvent, acetonitrile, $Fe(TPA)Cl_2$ 0.1 mM, $Zn(OTf)_2$ 0.2 mM, 15 min/scan, 298 K.